Appl Phys B (2011) 105:537–543
DOI 10.1007/s00340-011-4611-3

Applied Physics B
Lasers and Optics

Application of optical pyrometry for on-line monitoring in laser-cutting technologies

A.V. Dubrov · V.D. Dubrov · Y.N. Zavalov · V.Y. Panchenko

Received: 23 October 2010 / Revised version: 3 May 2011 / Published online: 8 July 2011

Abstract The results of measurement of fluctuations of brightness temperature T in the region of exposure to laser radiation of a 3 mm-thick steel plate are presented. The local luminosity along the cut-front was measured using two-color multichannel pyrometer. Cutting trials were carried out with CO_2 laser (10.6 μm, 1200 W) and fiber laser (1.07 μm, 1800 W). Special attention was given to the frequency range of temperature fluctuations above frequency of melt overflight, aiming on on-line monitoring applications. It is shown that local fluctuations of T are related to local melt's surface deformations due to unequal radiation absorption; thus the noise spectrum of T fluctuations reflects turbulent surface deformation, caused by gas jet and capillary waves. It is also shown that the thermo-capillary effect with capillary-wave turbulence generation can be observed in case of exposure to 10.6 μm radiation with a laser intensity of about 1 MW/cm^2. The power law of "−7/6" describes the spectrum of the T fluctuation variance in this case of anomalous absorption of radiation, and the standard deviation of T is in excess of 10 K for a frequency of 14 kHz. There is no such effect in case of fiber-laser radiation applying, and the source of the capillary waves is only forced low-frequency deformations of the melt surface. The standard deviation of T does not exceed 3 K on the frequency of 14 kHz, and above, and a power law of the spectrum fluctuation is described by about "−3" in that range.

A.V. Dubrov (✉) · V.D. Dubrov · Y.N. Zavalov · V.Y. Panchenko
Institute on Laser and Information Technology of Russian Academy of Science, 1 Svyatoozerskaya st., 140700 Shatura, Moscow Region, Russia
e-mail: dubrovav@gmail.com

1 Introduction

The technology of cutting sheet materials with gas lasers is currently widely spread. However, when this technological procedure is automated, upgrading of its quality and reliability presents an urgent problem. It has been suggested in [1, 2] that pulsations of brightness of thermal emission from the zone of laser beam action on metal should be measured with the aim of laser-cutting control, and a correlation between pulsations of emitted light brightness and averaged surface roughness has been revealed. Different methods for on-line monitoring of laser thermal effect on materials are studied currently to improve the quality of technological operations [3, 4]. Acoustic [5] and optical [6] methods of non-destructive testing were used. Papers [2, 6] display a relationship between the pulsation spectrum of metal melt heat emission and the striation frequency of the cut side edge. A system of laser-cutting process monitoring that uses data on radiation pulsation over three spectral bands has been suggested in [7], and it allows one to measure pulsations of brightness temperature. Paper [8] discusses an optical system representing an array of photo sensors to exert monitoring of the cavity processes in laser welding. It is also advised that optical fibers should deliver the luminous flux from the radiation zone to the photo sensors. The paper [9] describes the application of high speed photography to follow the dynamics of melt in the cutting area.

We have previously carried out comparison studies on the pulsation spectrum of integrated luminosity of emission from the laser-cutting zone [10], the spectrum of brightness temperature under two-color pyrometry [11], and the spectrum of the side edge roughness, resulting from laser cutting [12]. This paper reports the results of measuring by a four-channel two-color pyrometer of local brightness temperature pulsations in the region of exposure to laser radiation of 3 mm-thick steel plate.

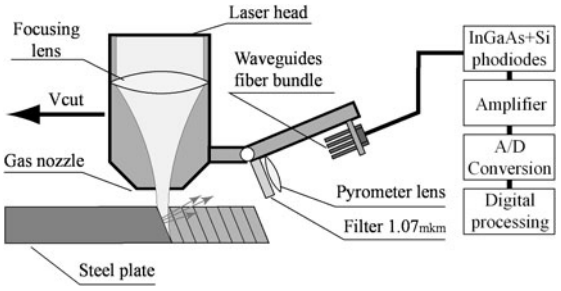

Fig. 1 Experimental set-up

2 Experimental set-up

The experimental set-up is shown schematically on Fig. 1. A portion of light emitted by a region of cut zone heated by laser radiation is converged by an optical lens and illuminates the end faces of four optical fibers located at an angle of ∼30° to the plane of the sheet as shown in Fig. 1. We used an optical filter in case of the fiber laser to avoid the influence of its radiation on the photodiodes. The light was delivered by an optical fiber (core diameter equals 62 μm) to the photodiodes. The photocurrents of the photodiodes are amplified, and then they were measured by the 14-bit data acquisition system. Photo-sensors of type K1713-05 [Hamamatsu] are used. This type of detector incorporates an infrared transmitted Si photodiode mounted over an InGaAs PIN photodiode along the same optical axis. The thermal radiance as local luminosity of the melt surface in this case lights the end face of the fiber. The illumination of the photodiode does not only depend on the temperature in the heated region, but on other factors as well, among them the area of melted material luminosity, the distance from source of thermal flux, the heated surface luminosity pattern, and the angular sensitivity of optical sensors. The employment of a lens in the pyrometer allows the spatial selectivity of measurements to be improved; the angle of arrival of light from local point of melt surface was increased, so the greater part of thermal radiance from local point gathers to the photo detector. The spectrum of light sensitivity of Si photodiode is estimated to be about 680 nm to 1050 nm, and the spectrum of light sensitivity of InGaAs photodiode is estimated to be about 960 nm to 1700 nm. The measurement of the brightness temperature applied the two-color method of pyrometry: the local brightness temperature defined in this case as a function of the ratio of photocurrents of two photodiodes with sensitivity to neighboring regions of the near infra radiation spectrum. This method reduces the influence of intervening factors on the source brightness.

2.1 Laser cutting; CO_2 laser

The experiments make use of a "Trumatic 2530" machine [Trumpf Gmbx] equipped with a TLF 1500 CO_2 laser. The output power of 10.6 mkm laser radiation was set on level of 1200 W. Cutting of a low-carbon steel sheet 3 mm thick in oxygen as an assist gas was made with "optimal" cutting parameters: the nozzle of ∅0.8 mm was located at 0.7 mm from the sheet upper surface; the lens focus of 127 mm was 0.4 mm above the sheet surface. The cutting speed was varied from 35 to 60 mm/s in the experiments on cutting different specimens, the "optimal" speed being 50 mm/s. Oxygen was used as an assist gas, its pressure being varied from 1 bar to 2.5 bars. The local brightness temperature has been taken for different values of depth in the channel: 0.4 mm, 1.2 mm, 2 mm and 2.8 mm.

Figure 2 illustrates the temporary behavior of the brightness temperature T^* measured on different depths of the cut front, where the time scale is changed in the diagrams. The melt velocity estimation has been made, suggesting that local temperature minimum moves down with that velocity. We got the value of 8 meters per second. So a third of a millisecond is the time-of-flight scale. The estimation of melt thickness is

$$\delta = \frac{V_{cut}}{V_{melt}} \cdot h \approx 20\ \mu\text{m} \tag{1}$$

2.2 Laser cutting; ytterbium-doped fiber laser

Another series of experimental cutting of a low-carbon steel sheet of 3 mm thick was made, Fig. 3. There was used ytterbium-doped fiber laser YLS-3000 [IPG Photonics]. The output power of 1.07 mkm laser radiation was 1800 Watts and oxygen was used as an assist gas. The "optimal" cutting parameters were thus established: the nozzle of ∅1.2 mm was located at 0.3 mm from the sheet upper surface; the lens focus of 127 mm was 0.3 mm below the sheet surface. The cutting speed was varied from 30 to 60 mm/s in the experiments on cutting different specimens; the recommended speed for 3 mm thick of metal plate being 40 mm/s. The pressure of oxygen employed as an assist gas was 4 bar. The local brightness temperature has been taken for different values of depth of luminosity region: 0.6 mm, 1.2 mm, 1.8 mm and 2.4 mm. Figure 4 illustrates the temporary behavior of the brightness temperature T^* measured on depth 2.4 mm.

2.3 The spectrum of variance of brightness temperature T^*

The procedure of data processing has been earlier described in [10]. Averaging power spectra of pulsation makes possible enhancing the relative amplitude of resonance oscillations in the fluctuation spectrum against the background of random oscillations. The sections of one "long" realization, $N = 32$ or 64, were averaged based on ergodic theorem. Figure 5(a) displays the spectrum of standard deviation of T^* in case of CO_2 laser with output laser radiation

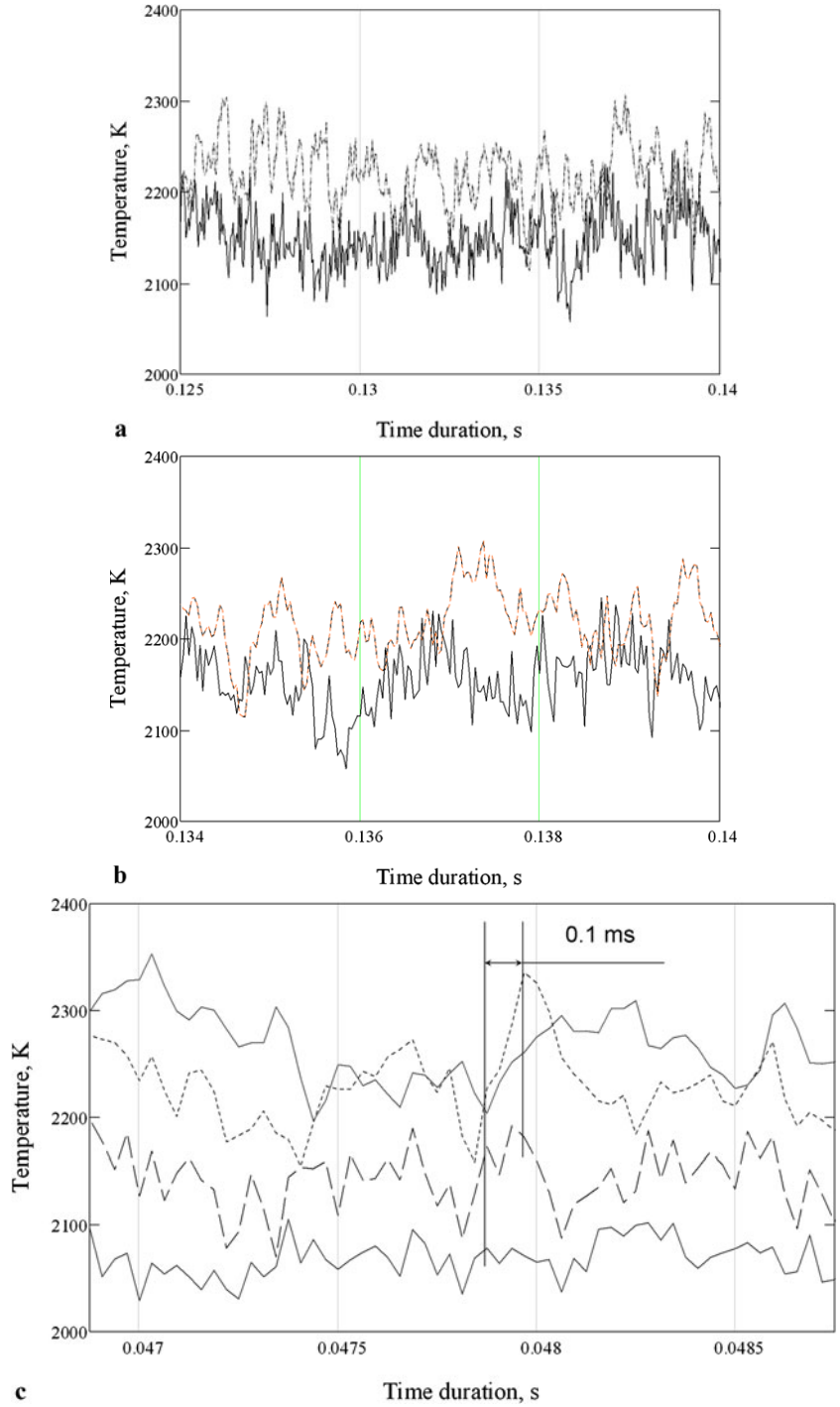

Fig. 2 Temporal behavior of brightness temperature T^* on different depths. Cutting with CO_2 laser. The cutting velocity is 50 mm/s, pressure of oxygen is 1 bar. (**a**) Depths: 1.2 mm (*solid line*) and 2.8 mm. (**b**) Depths: 1.2 mm (*solid line*) and 2.8 mm. (**c**) Depths: 0.4 mm (*solid line*), 1.2 mm, 2 mm and 2.8 mm (*solid line*) from *bottom* to *top*

of 10.6 μm wavelength corresponding to experimental estimation of variance spectrum $\overline{D_\omega^T}$. Similar dependences have been obtained in case of cutting by fiber laser; one of them is shown on Fig. 5(b)).

3 Theoretical background

To utilize the spectral dependences obtained, it is necessary to find equations that link the unsteady temperature behavior with processes of melt formation and melt removing. Measurements of pulsations of brightness temperature in the frequency range below 2 kHz were performed in our earlier studies [11] for cutting mild-steel sheets of 6 and 10 mm thickness. Quasi-resonance spectral peaks were observed and it was shown that these local maximums in T^* pulsations spectrum were related to roughness spatial spectrum of forming side edge. Low-frequency fluctuations of T^* were explained in this case by relaxation-oscillation movements

Fig. 3 Photo of the experimental set-up for 1.07 micron radiation cutting with ytterbium-doped fiber laser

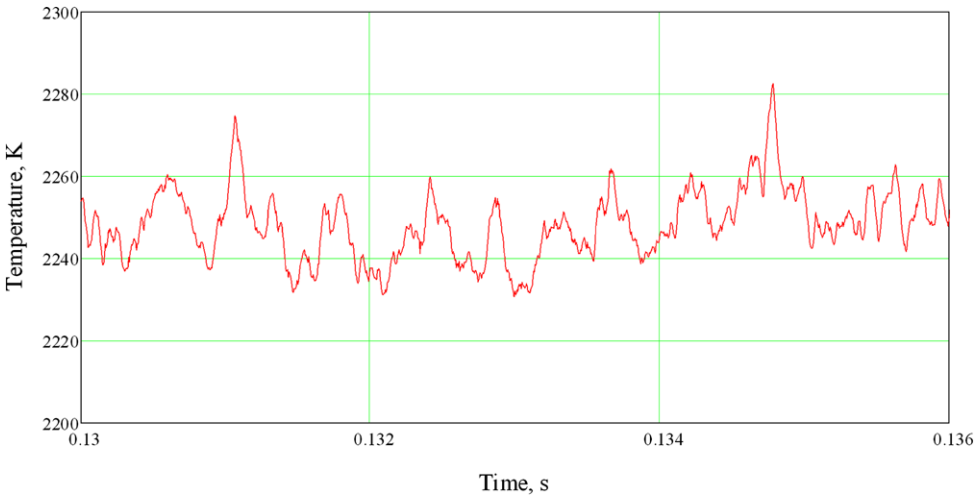

Fig. 4 Brightness temperature T^* behavior. Mild steel of 3 mm thickness, the cutting velocity is 35 mm/s, pressure of oxygen is 4 bar

of cut front relative to laser beam. In this paper special attention was given to fluctuation frequency range above frequency of melt overflight (∼3 kHz) aiming on-line monitoring applications. If we consider time intervals below time of melt-flight through sample thickness, the small spatial scale T^* fluctuations should be related to unsteadiness of melt flow with regard to gas jet forcing. There are many papers discussing these complicated processes.

It was shown [13] that stream is necessarily stratified into several layers by depth. Estimation of near-surface layer velocity was performed in (1). Deeper layers are slower and much deeper. Furthermore, high speed frames [9] demonstrated that stream surface becomes deformed; stream consistently changes its behavior distorting smooth surface with further splitting into separate jets and drops.

One needs to appreciate the feature of turbulent molten metal stream. Metals and molten metals are characterized by high thermal conductivity. The Prandtl number for metals is $\mathrm{Pr} = \nu/\chi \ll 1$ and typical value for steel is $\mathrm{Pr} \approx 1/16$. Whereas the power law of velocity pulsations is $\omega^{-5/3}$ for inertial range of Kolmogorov turbulence (ω is a cyclic frequency), the local temperature pulsations have a sharp decay with frequency rise: $\sim\omega^{-17/3}$ [14]. The power law of temperature pulsations in the viscous range is sharper: ω^{-7}. So high-frequency pulsations of temperature in volume of the melt flow are negligible, and other reasons of the temperature T^* pulsations, appearing in the experiment, should be found. We relate these pulsations with melt surface deformation.

The melt surface temperature is determined not only by convectional melt flow and heat conductivity into solid, but primarily in processes of local absorption of laser radiation, Fig. 6. Local heating depends on conditions of irradiation by laser light, such as local intensity, surface inclination to direction of beam propagation; furthermore heat conductivity could degrade with convex surface. Assume that the deviation from a stationary position of the free surface of the melt determines local temperature fluctuations, caused primarily by local peculiarities of the laser radiation absorption.

Thus, the variance spectrum D_ω^T of temperature of luminous surface could be related with energy spectrum of surface deformation, caused by local non-uniformity of surface tension. Two more spectral ranges can be selected as a re-

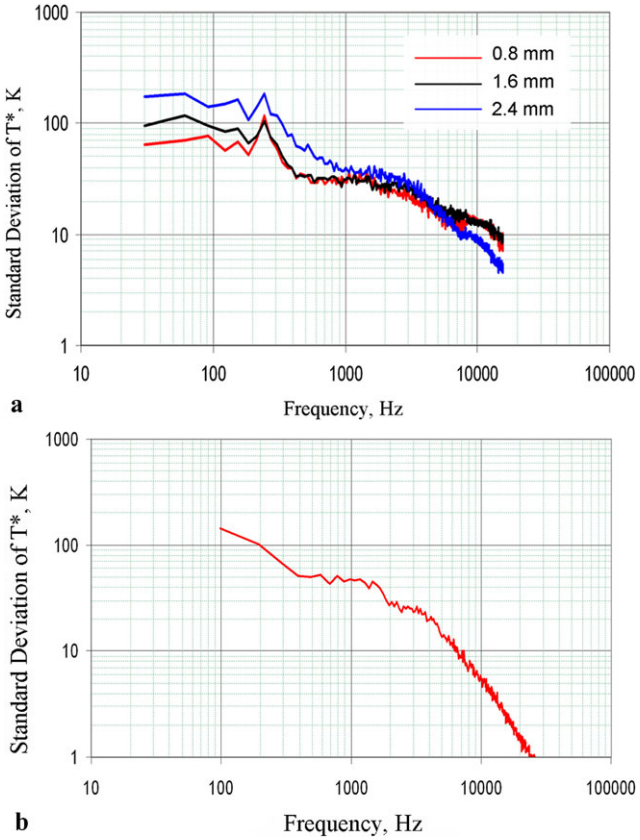

Fig. 5 Spectra of standard deviation of brightness temperature T^*. (**a**) CO_2 laser-cutting velocity is 43 mm/s, pressure of oxygen is 2.5 bar. (**b**) Cutting with ytterbium-doped fiber laser. Parameters as for Fig. 4

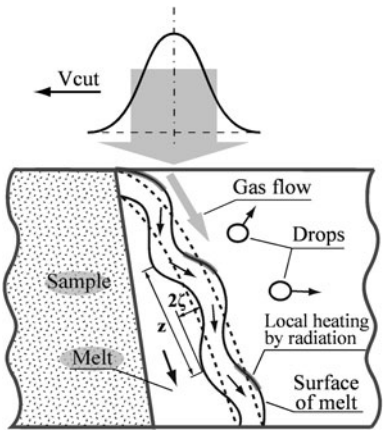

Fig. 6 Scheme of radiation action on metal

sult of discussion in addition to relaxation-oscillation movements of a cut front considered previously.

First, there is the range of 3 kHz (frequency of melt overflight) to 7 kHz (capillary-wave length is near 300 μm), the surface tension energy is insignificant compared to energy of forced turbulent pulsation. So the temperature pulsations are caused by gas jet energy injection due to macro deformation of melt surface. For developed turbulence:

$$D_\omega^T \sim C \cdot \omega^{-5/3}, \tag{2}$$

where C is a function of the gas pressure at the nozzle inlet.

At the second range, generation and propagation of capillary waves become significant. Surface tension σ and thermal dependence $\partial\sigma/\partial T$ (for most metals and alloys $\partial\sigma/\partial T < 0$) play a key role at small scales. The capillary-wave turbulence phenomenon was considered in [15], and some new results were presented [16, 17]. Dispersion equation for capillary waves is

$$\omega^2 = k^3(\sigma/\rho). \tag{3}$$

We take into account in estimations next data for liquid mild steel: $\sigma \approx 1.5$ N/m, melt density $\rho \approx 7000$ kg/m^3, $\partial\sigma/\partial T \approx -0.6$ mN/(m · K). So, we estimate the Marangoni number as Ma ≈ 10. The phase velocity of capillary waves varies (2–16) m/s in a frequency range of 7 kHz to 3 MHz for mild steel, the relative wavelength varies in a range of (300–5) μm, the case of "deep" liquid was calculated.

Correlation function of the deviation ξ of the surface of the melt from the stationary position is determined by

$$\Gamma(\tau) = \langle \xi(t) \cdot \xi(t+\tau) \rangle. \tag{4}$$

The Fourier transform of the correlation function associated with the spectrum of capillary-wave energy by the following relation taken into account dispersion equation (1):

$$\Gamma_\omega = E_\omega \cdot \omega^{-4/3}, \quad \text{or for wave number } k,\ \Gamma_k = E_k \cdot k^{-2}. \tag{5}$$

There is the following power dependence of the energy distribution on wave number of the capillary waves in the inertial range according to the theory of weak turbulence [15]:

$$E_k \sim k^{-9/4}. \tag{6}$$

Consequently, the Fourier transform of the correlation function has the frequency dependence in the inertial range:

$$\Gamma_\omega \sim \omega^{-17/6}, \quad \text{or for wave numbers, } \Gamma_k \sim k^{-17/4}. \tag{7}$$

The case of an ensemble of capillary waves forming by forced low-frequency deformations of melt surface was studied e.g. in [18]. Experimental estimation of spectrum of energy density of capillary waves for this case is $\Gamma_\omega = \omega^{-m}$, where $m = 2.8$–3.3.

Where forming an inverse cascade of wave turbulence, the energy of small-scale capillary waves is transmitted in processes of decay instability, $\vec{k} = \vec{k}_1 + \vec{k}_2$, $\omega = \omega_1 + \omega_2$, forming longer waves [15]:

$$\Gamma_\omega = \omega^{-7/6}, \quad \text{or} \quad \Gamma_k \sim k^{-7/4} \tag{8}$$

To estimate temperature deviation from the stationary value assume in the first approximation: $D_\omega^T \sim \Gamma_\omega$ for individual spectral components of a continuous spectrum of fluctuations of physical parameters.

4 Results and discussion

Based on the data obtained, the function $\Omega = \overline{D_\omega^T} \cdot \omega^2$ was calculated. The function Ω has a maximum on the boundary between inertial and viscous ranges in case of hydrodynamic developed turbulence, as shown in Fig. 7(a), where results of experiment with fiber laser are presented. But we see Ω's growth in viscous range, while T^* pulsation frequency rises in case of a CO_2 laser, Fig. 8(a) and (b).

In Figs. 7(b) and 8(b), the dependence of the compensated function $Y(k) = \overline{D_k^T} \cdot k^{7/4}$ is presented. The function $Y(k)$ should have horizontal line as approximation within inertial range of capillary-wave turbulence. As we see, this prediction matches the CO_2 experimental data, in contrast to data obtained in fiber-laser experiments.

An example of a compensated function $Z(k) = \overline{D_k^T} \cdot k^{17/4}$ plotting is presented in Fig. 7(c). In case of fiber laser, as follows from the figure, in the range of turbulent flow energy dissipation, forming capillary-wave's ensemble leads to small-scale temperature pulsations, so variance spectrum is $D^T(k) \sim k^{-17/4}$.

In case of using CO_2 laser with focus intensity of 1 MW/cm^2 (estimation is done with laser power 1200 W and a lens with $F = 127$ mm) special regime of small-scale capillary-wave generation occurs. These waves form a so-called capillary-wave turbulence spectrum.

What process could be the source of small-scale capillary waves? It is assumed that having such intensity on metal surface, 1 MW/cm^2, and wavelength 10.6 μm, threshold of thermo-capillary instability (TCI) development is exceeded. As shown in [19], the main reason of thermo-capillary effect (TCE) development is the presence of a thermal dependence of surface tension. To compare the phase velocity of capillary waves with melt flow velocity we calculated that capillary wave of 24 μm length has the phase velocity of 8 m/s that is same as we takes into account in (1) for melt flow velocity. We suppose that the vertical (along cutting front) component of generated thermo-capillary waves is directed upstream, as it is considered in [19] for the case of thermo-capillary waves with wavelength longer than the laser wavelength. Thus capillary-wave lifetime is increased due to the direction of propagation of generated thermo-capillary waves that reserves quite some time to develop and decay generated waves in processes of capillary turbulence. The interaction time to form a capillary cascade is estimated as several milliseconds [20].

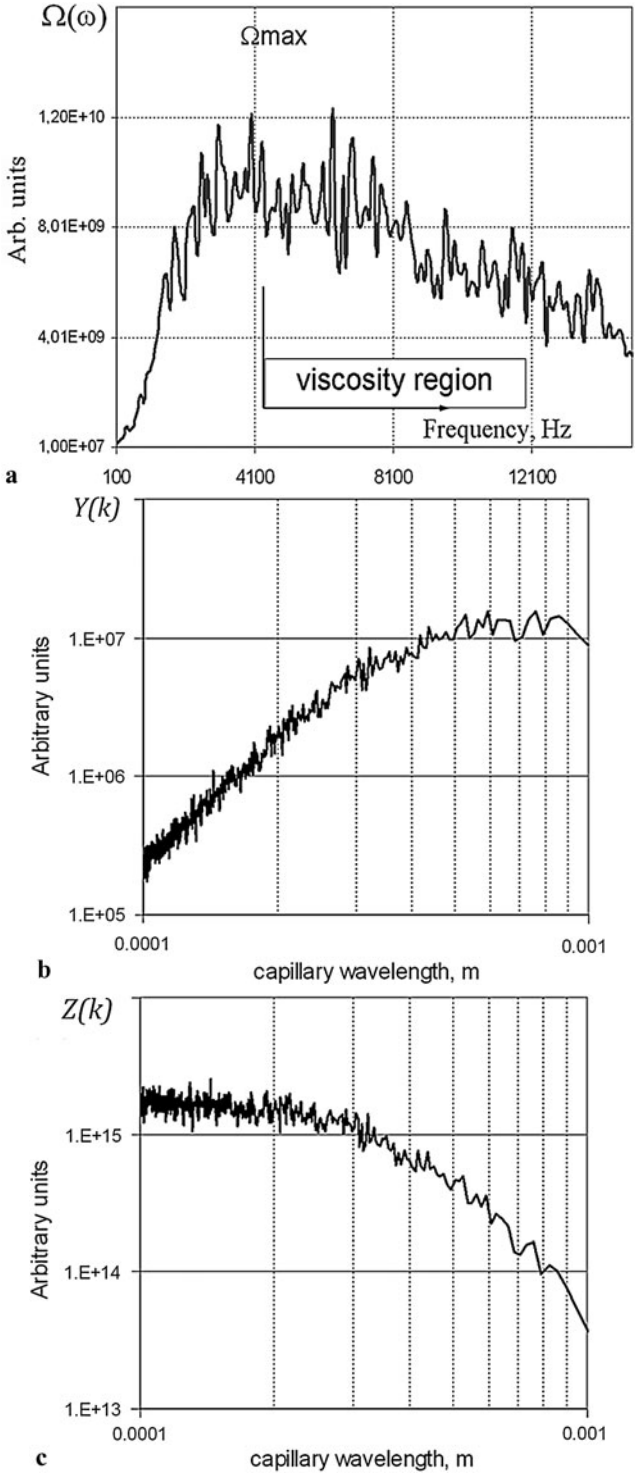

Fig. 7 Spectra of auxiliary functions, ytterbium-doped fiber laser, 1.07 μm output radiation; the cutting velocity is 35 mm/s, pressure of oxygen is 4 bars

The threshold of TCI development depends on wavelength of laser radiation because implementation of same spatial gradients on small-scales is more complex. Taking into account the power-like dependence of spatial (along

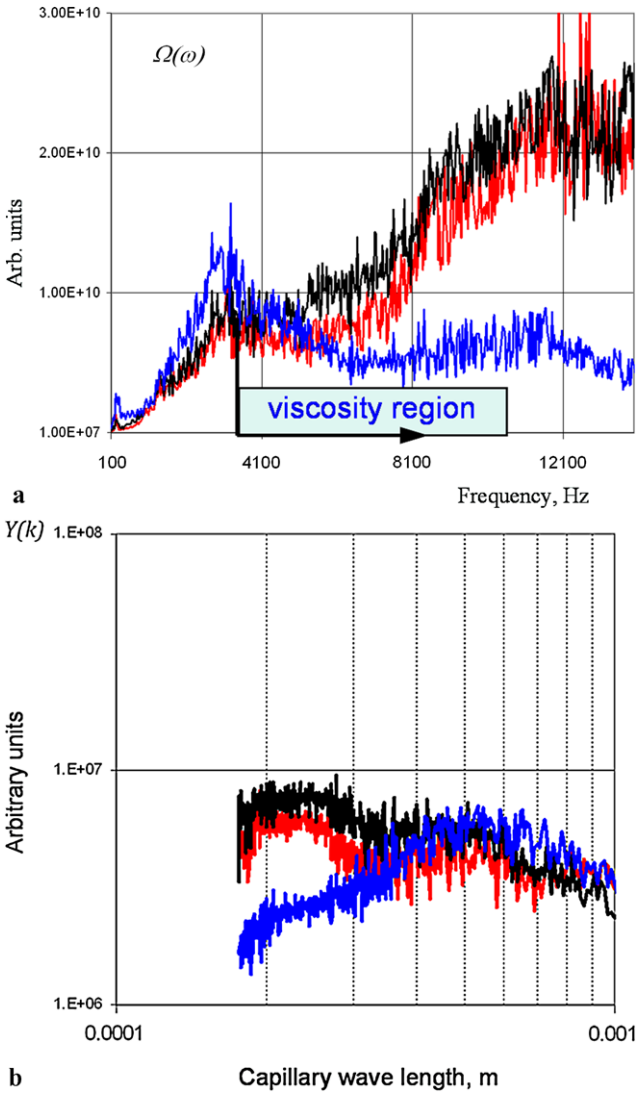

Fig. 8 The spectra of auxiliary functions, CO_2 laser with 10.6 μm wavelength radiation; the cutting velocity is 43 mm/s, pressure of oxygen is 2.5 bar

the surface) gradient of temperature on the spatial scale allows us to explain the absence of TCE in experiments with 1.07 μm wavelength fiber laser and same intensity level. The dependence of the TCI threshold on the laser wavelength was estimated theoretically before in [19].

5 Conclusion

It is shown that local fluctuations of T^* are related to local melt's surface deformations due to unequal radiation absorption. The noise spectrum of T^* fluctuations reflect turbulent surface deformation which can be of two types in this case: caused by gas jet and capillary waves. It is also shown that in case of exposure to 10.6 μm radiation the thermo-capillary effect with capillary-wave turbulence generation can be observed. This nonlinear effect of laser radiation absorption was observed with a laser intensity of about 1 MW/cm^2. There is a range with a power law of "−7/6" in the T^* fluctuation variance spectrum in this case, and the standard deviation of T^* on frequency of 14 kHz is in excess of 10 K. There is no such effect in case of using fiber-laser radiation, and the source of capillary waves is only forced low-frequency deformations of melt surface. The standard deviation of T^* does not exceed 3 K on the frequency of 14 kHz and above, and the power law of the fluctuation variance spectrum is described by about "−3" in that range.

References

1. M. Hansmann, I. Decker, J. Ruge, in *Power Beam Technology*, Brighton, England (1986), pp. 440–445
2. I. Decker, H. Heyn, D. Martinen, H. Wohlfahrt, Proc. SPIE **3097**, 29 (1997)
3. J.R. Duflou, E.F. Sichani, J. De Keuster, J.-P. Kruth, in *ICALEO Proceedings*, Orlando, USA, vol. 102 (2009), pp. 527–536
4. F. Bardin, S. Morgan, S. Williams, R. McBride, A.J. Moore, J.D.-C. Jones, D.P. Hand, Appl. Opt. **44**, 6841 (2005)
5. J. De Keuster, J.R. Duflou, J.-P. Kruth, Int. J. Adv. Manuf. Technol. **35**, 115 (2007)
6. P. Sforza, V. Santecesaria, Proc. SPIE **2207**, 836 (1994)
7. P. Sforza, D. de Blasiis, V. Lombardo, Proc. SPIE **3097**, 97 (1997)
8. T. Engel, M. Kane, J. Fontaine, Proc. SPIE **3097**, 727 (1997)
9. I. Miyamoto, H. Maruo, Weld. World **29**, 283 (1991)
10. R.V. Grishaev, V.D. Dubrov, N.G. Dubrovin, Y.N. Zavalov, J. Guangdong Non-Ferrous Met. **3**, 635 (2005)
11. V.S. Golubev, A.V. Dubrov, Yu.N. Zavalov, V.D. Dubrov, in *Theses of 5th International Conference on Advanced Optoelectronics and Lasers (CAOL'2010)*, Sevastopol, Ukraine, 10–14 Sept. (2010), pp. 182–184. IEEE CN: CFP10814-PRT
12. V.S. Golubev, R.V. Grishaev, V.D. Dubrov, N.G. Dubrovin, Yu.N. Zavalov, in *Theses of XIId International Conference on Physical and Chemical Processes in Selection of Atoms and Molecula*, Zvenigorod, Russia, 31 March–4 Apr 2008 (TsNIIAtomInform, Moscow, 2008), pp. 255–260. ISBN 978-5-89513-133-6, in Russian
13. V.S. Golubev, Proc. SPIE **2713**, 219 (1995)
14. P.G. Frick, *Turbulence: Method and Approach* (Moscow, 2003), in Russian
15. V.E. Zakharov, V.S. L'vov, G. Falkovich, *Kolmogorov Spectra of Turbulence I: Wave Turbulence*, Springer Series in Nonlinear Dynamics (Springer, Berlin, 1992)
16. G.V. Kolmakov, A.A. Levchenko, M.Yu. Brazhnikov, L.P. Mezhov-Deglin, A.N. Silchenko, P.V.E. McClintock, Phys. Rev. Lett. **93**, 074501 (2004)
17. E. Falcon, C. Laroche, Phys. Rev. Lett. **98**, 094503 (2007)
18. M.Yu. Brazhnikov, A.A. Levchenko, L.P. Mezhov-Deglin, Instrum. Exp. Tech. **45**, 758 (2002)
19. N.I. Koroteev, V.I. Emel'yanov, V.N. Seminogov, S.A. Akhmanov, Usp. Fiz. Nauk **28**, 1084 (1985)
20. V.E. Zakharov, N.N. Filonenko, J. Appl. Mech. Tech. Phys. **5**, 310 (1967)